

Spectral Properties and Low-Dimensional Description of Loop and Recycle Reactors

Imran Alam and Vemuri Balakotaiah

Dept. of Chemical and Biomolecular Engineering, University of Houston, Houston, TX 77204

DOI 10.1002/aic.14097

Published online April 8, 2013 in Wiley Online Library (wileyonlinelibrary.com)

The spectral properties of the discrete and continuous convection and convection-diffusion operators with loop or recycle boundary condition are analyzed. It is shown that the spectral properties of these nonsymmetric operators are closely related to the theory of circulant (Toeplitz) matrices and the complex Fourier series, respectively. Although there may be many complex eigenvalues, the smallest eigenvalue is real and approaches zero as the loop circulation or recycle ratio increases. This property is used to simplify nonlinear diffusion-convection-reaction models of loop and recycle reactors to obtain two-mode low-dimensional averaged models that are accurate in the limit of large recycle ratio. Explicit expressions for the two mixing coefficients that relate the two concentration modes and their dependence on various inlet conditions are also derived. Finally, the application of the low-dimensional models to determine the impact of macromixing on the conversion, yield, and selectivity for the case of nonlinear kinetics is illustrated. © 2013 American Institute of Chemical Engineers AIChE J, 59: 3365-3377, 2013

Keywords: mathematical modeling, mixing, multiscale modeling, reactor analysis

Introduction and Literature Review

The use of recycle streams is common in many chemical processes, as it facilitates moderation of temperature gradients, reuse of the catalyst, inhibition of undesired side reactions, circulation of the working fluid, and so forth. In a recycle reactor, a fraction of the product stream is mixed with the feed stream, whereas in a loop reactor, the reactants can enter and the products leave a circulating loop. In a loop reactor, the reaction can occur throughout the loop, whereas in a recycle reactor, it is generally assumed that no reaction occurs in the recycle stream and that the delay is negligible. Loop and recycle reactors are used to carry out highly exothermic reactions and are preferred over stirred tank reactors when a large heat-transfer area per unit volume is desired. Many liquid-phase polymerization reactions with a suspended catalyst (slurry) are carried out in loop reactors. Loop and recycle reactors with a large recycle ratio are also used in the laboratory to determine the kinetics of many solid catalyzed reactions.

Despite their extensive use, the mathematical theory of loop and recycle reactors has not been examined in the literature. One exception (and the motivation for this work) is the earlier work of Schmeal and Amundson¹ and Luss and Amundson.² Following the earlier work of Nagiev³ on the theory of recycle processes, Luss and Amundson² examined the stability of adiabatic loop tubular reactors using a graphical approach based on the heat generation and removal curves. The impact of recycle on the transient behavior of a recycle reactor with linear kinetics

was analyzed by Schmeal and Amundson¹ using the argument principle. While there is extensive literature on the steady state and transient behavior of convection dominated (parabolic and hyperbolic) systems, except for the studies mentioned earlier, it appears that the literature dealing with the analysis of the same systems in the presence of recycle is limited. It should also be pointed out that while the application of matrix and linear operator methods is well established in the chemical engineering literature (Amundson⁴; Ramkrishna and Amundson⁵; Ramkrishna and Amundson⁶; and Kevrekidis⁷), there appears to be very limited application of the theory of circulant (and Toeplitz) matrices.

The main goal of this work is to analyze the spectral properties of the continuous and discrete convection and convection-diffusion operators with loop or recycle boundary condition. We show that the spectral properties are closely related to the theory of complex Fourier series and circulant (Toeplitz) matrices, respectively. We use the property that the smallest eigenvalue is real and approaches zero as the recycle ratio increases, to simplify the nonlinear models of loop and recycle reactors to a low-dimensional form consisting of ordinary differential and algebraic equations. We illustrate the application of the low-dimensional models to determine the impact of macromixing that occurs due to the entrance and exit of various feed and product streams at different locations in the loop and at different concentrations, on the conversion, yield, and selectivity for the case of isothermal nonlinear reaction kinetics.

Spectral Properties of the Convection Operator

In this section, we consider the spectral properties of the continuous and discrete convection operator with recycle/loop boundary condition.

Correspondence concerning this article should be addressed to V. Balakotaiah at bala@uh.edu.

The continuous convection operator, $\frac{d}{dx}$

The simplest model of a recycle reactor is that of an isothermal tubular plug flow reactor with a nonlinear reaction and is governed by the following partial differential equation for the reactant concentration

$$\frac{\partial C}{\partial t'} + \frac{(q_F + Q_R)}{A_c} \frac{\partial C}{\partial x'} = -R'(C); \quad 0 < x' < L, \quad t' > 0 \quad (1)$$

where q_F (Q_R) is the volumetric flow rate of the feed (recycle) stream, A_c is the tube cross-sectional area, and $R'(C)$ is the reaction rate (or more precisely, the rate of disappearance of the limiting reactant). The recycle boundary condition is given by an algebraic equation representing the species mass (or mole) balance at the mixing point at which the feed and the recycle streams combine

$$q_F C_F(t') + Q_R C(L, t') = (q_F + Q_R) C(0, t'). \quad (2)$$

The model is completed by an appropriate initial condition. Defining dimensionless variables

$$\begin{aligned} x = \frac{x'}{L} \quad t = \frac{q_F t'}{A_c L} \quad c = \frac{C}{C_R} \quad c_m^{\text{in}}(t) = \frac{C_F \left(\frac{A_c L t}{q_F} \right)}{C_R} \\ Da = \frac{A_c L R'(C_R)}{q_F C_R} \quad r(c) = \frac{R'(C_R c)}{R'(C_R)} \quad \epsilon = \frac{q_F}{Q_R} \end{aligned} \quad (3)$$

the model may be expressed as

$$\frac{\partial c}{\partial t} + \left(\frac{1 + \epsilon}{\epsilon} \right) \frac{\partial c}{\partial x} = -Dar(c); \quad 0 < x < 1, \quad t > 0 \quad (4)$$

$$\epsilon c_m^{\text{in}}(t) + c(1, t) = (1 + \epsilon)c(0, t) \quad (5)$$

$$c(x, 0) = c_0(x) \quad (6)$$

where $c_0(x)$ is the function specifying the initial condition. Here, C_R (C_F) is a reference (feed) concentration, ϵ is a small parameter representing the ratio of feed to recycle flow rate (or the ratio of the characteristic loop circulation time to the residence time). It is related to the traditionally used fractional recycle (f_R) by $f_R = \frac{Q_R}{(q_F + Q_R)} = \frac{1}{1 + \epsilon}$ and recycle ratio (R) by $R = \frac{Q_R}{q_F} = \frac{1}{\epsilon}$. We note that though the partial differential equation 4 is hyperbolic, the above model does not define a Cauchy (initial value) problem due to the recycle boundary condition Eq. 5, except in the limit of $\epsilon \rightarrow \infty$ (no recycle). The focus of this work is the limit $\epsilon \rightarrow 0$, corresponding to a large recycle ratio. In this limit, we rewrite the model defined by Eqs. 4 and 5 as

$$\frac{\partial c}{\partial x} = -\epsilon \left[\frac{\partial c}{\partial t} + Dar(c) + \frac{\partial c}{\partial x} \right]; \quad 0 < x < 1, \quad t > 0 \quad (7)$$

$$c(1, t) - c(0, t) = \epsilon [c(0, t) - c_m^{\text{in}}(t)]. \quad (8)$$

For the case of a loop reactor (shown schematically in Figure 1a), taking $x' = 0$ as the point at which the reactant enters and $x' = L_1$ as the point at which the product leaves the loop, the model is described by

$$\frac{\partial C}{\partial t'} + \frac{(q_F + Q_R)}{A_c} \frac{\partial C}{\partial x'} = -R'(C); \quad 0 < x' < L_1, \quad t' > 0 \quad (9)$$

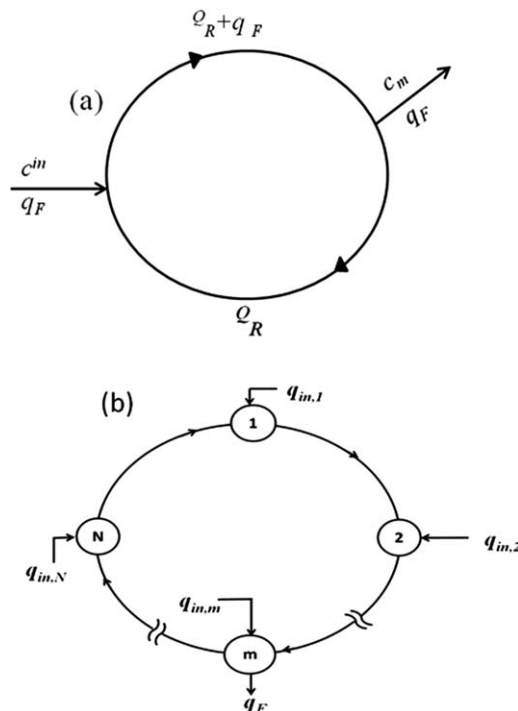


Figure 1. A schematic diagram of the loop reactor in the (a) continuous and (b) discrete case.

$$\frac{\partial C}{\partial t'} + \frac{Q_R}{A_c} \frac{\partial C}{\partial x'} = -R'(C); \quad L_1 < x' < L, \quad t' > 0 \quad (10)$$

with the same boundary condition as that given by Eq. 2. In dimensionless form, the model for the loop reactor may be written as

$$\frac{\partial c}{\partial x} = -\epsilon f(c, x, t); \quad x \in [0, \theta) \cup (\theta, 1), \quad t > 0 \quad (11)$$

$$f(c, x, t) = \begin{cases} \frac{\partial c}{\partial t} + Dar(c) + \frac{\partial c}{\partial x}, & 0 < x < \theta \\ \frac{\partial c}{\partial t} + Dar(c), & \theta < x < 1 \end{cases} \quad (12)$$

with the same boundary condition as Eq. 8 and $\theta = L_1/L$.

Examining the leading order spatial operator for both models, we note that the relevant eigenvalue problem for the convection operator is defined by

$$\mathcal{L}w \equiv \frac{dw}{dx} = \lambda w; \quad w(1) - w(0) = 0 \quad (13)$$

We note that this operator is not symmetric and the adjoint operator with respect to the usual inner product

$$\langle w(x), v(x) \rangle = \int_0^1 w(x) \overline{v(x)} dx \quad (14)$$

is given by

$$\mathcal{L}^* v \equiv -\frac{dv}{dx}; \quad v(0) - v(1) = 0 \quad (15)$$

The characteristic equation for the eigenvalue problem, Eq. 13 is

$$h_c(\lambda) \equiv \exp(\lambda) - 1 = 0 \quad (16)$$

and the spectrum of \mathcal{L} is given by

$$\lambda_0 = 0 \quad (17)$$

$$\lambda_m = 2m\pi i; i = \sqrt{-1}; m = \pm 1, \pm 2, \dots \quad (18)$$

Thus, in the limit of large recycle ratio, the convection operator with loop/recycle boundary condition has one (simple) zero eigenvalue (and a constant eigenfunction, which may be taken as unity) and an infinite number of imaginary eigenvalues which are integer multiples of $2\pi i$, and complex valued eigenfunctions. It is easily seen that for finite but small ϵ , this scale separation persists. For example, for the case of a recycle reactor, it is easily seen that for small ϵ , the spectrum of the perturbed operator

$$\mathcal{L}(\epsilon)w \equiv (1 + \epsilon)\frac{dw}{dx}; \quad w(1) - (1 + \epsilon)w(0) = 0 \quad (19)$$

is given by

$$\lambda_0(\epsilon) = (1 + \epsilon)\ln(1 + \epsilon) = \epsilon + O(\epsilon^2) \quad (20)$$

$$\lambda_m(\epsilon) = (1 + \epsilon)\ln(1 + \epsilon) \pm 2m\pi i = \epsilon \pm 2m\pi i + O(\epsilon^2) \quad (21)$$

Thus, for any finite ϵ , all the eigenvalues, except the smallest in magnitude, are complex. Further, the smallest (in magnitude) eigenvalue $\lambda_0(\epsilon)$ approaches zero as $\epsilon \rightarrow 0$. While the (real valued) solution of the transient model (for the case of linear kinetics or no reaction) may be expressed in terms of the complex valued eigenfunctions (using the complex form of the finite Fourier transform), this solution is not useful from a practical standpoint, as the convergence is very slow. However, this complex algebra can be avoided, and the degrees of freedom of the model can be reduced if we restrict the solutions to the practical case of small ϵ .

Defining the average concentration by

$$\langle c \rangle(t) = \int_0^1 c(x, t) dx \quad (22)$$

the loop or recycle reactor models can be integrated in the limit of $\epsilon \rightarrow 0$, to obtain the low-dimensional (lumped) ideal Continuous-flow Stirred Tank Reactor (CSTR) model

$$\frac{d\langle c \rangle}{dt} = c_m^{\text{in}}(t) - \langle c \rangle - \text{Dar}(\langle c \rangle); t > 0 \quad (23)$$

$$\langle c \rangle(t=0) = \langle c_0 \rangle \quad (24)$$

We show in the next section that this averaging or dimension reduction can be continued for small but finite values of ϵ .

The discrete convection operator

We now consider the discrete convective loop consisting of N identical cells of equal volume V_c , as shown in Figure 1b. On the main convective flow (Q_R), we superimpose weak flows that correspond to the entry or exit of one or more streams containing reactants and/or products in any particular cell. Although our approach is valid for cells of unequal volume (with a volume weighted average inner product) and an arbitrary arrangement, where each cell may be coupled to any number of other cells, for the sake of

algebraic simplicity, we confine the treatment below to the special case of the convective loop consisting of identical cells (Figure 1b) and one exit stream from cell m ($1 \leq m \leq N$). Further, we assume a constant density system so that the exit volumetric flow rate (q_F) from cell m is equal to the sum of all the volumetric flow rates of the feed streams entering the various cells. Using the same notation as in the previous section, the reactant species balance in vector form gives the model

$$\mathbf{Q}_R \mathbf{C} = V_c \left[-\frac{d\mathbf{C}}{dt'} - \mathbf{R}'(\mathbf{C}) \right] + \mathbf{q}_{\text{in}} \mathbf{C}_{\text{in}}(t') - \mathbf{q}_e \mathbf{C} \quad (25)$$

with an appropriate initial condition. Here, \mathbf{C} (\mathbf{C}_{in}) is the vector representing the species (inlet) concentrations in various cells, \mathbf{q}_{in} is a diagonal matrix representing the inlet volumetric flow rates to the cells, \mathbf{q}_e is a matrix representing the auxiliary flow rates leaving (or entering) various cells (excluding the main convective flow), and \mathbf{Q}_R is the $N \times N$ matrix (loop or cell connectivity) operator defined by

$$\mathbf{Q}_R = Q_R \begin{pmatrix} 1 & 0 & \dots & 0 & -1 \\ -1 & 1 & \dots & 0 & 0 \\ 0 & -1 & \dots & 0 & 0 \\ \vdots & \vdots & \ddots & \vdots & \vdots \\ 0 & 0 & \dots & -1 & 1 \end{pmatrix} \quad (26)$$

and $\mathbf{R}'(\mathbf{C})$ is the vector of reaction rates. The discrete loop operator \mathbf{Q}_R is a circulant matrix, which is a special case of a Toeplitz matrix (Aldrovandi⁸). We note that all the rows and all the columns of \mathbf{Q}_R sum to zero, hence a zero eigenvalue is guaranteed. However, as in the case of continuous operator, \mathbf{Q}_R is not symmetric with respect to the usual inner product in $\mathbb{R}^N/\mathbb{C}^N$. Defining dimensionless variables

$$t = \frac{q_F t'}{NV_c}, \quad \mathbf{c} = \frac{1}{C_R} \mathbf{C}, \quad q_F = \sum_{j=1}^N q_{\text{in},j} \quad (27)$$

$$Da = \frac{NV_c R'(C_R)}{q_F C_R}, \quad r_j(c_j) = \frac{R'(C_R c_j)}{R'(C_R)}, \quad \epsilon = \frac{q_F}{Q_R}$$

$$\alpha_{\text{in},j} = \frac{q_{\text{in},j}}{q_F}, \quad \alpha_e = \frac{1}{q_F} \mathbf{q}_e, \quad \mathbf{c}_{\text{in}}(t) = \frac{1}{C_R} \mathbf{C}_{\text{in}} \left(\frac{V_c N t}{q_F} \right) \quad (28)$$

the model defined by Eq. 25 may be written as

$$\mathbf{A} \mathbf{c} = \epsilon \left[-\frac{d\mathbf{c}}{dt} - \text{Dar}(\mathbf{c}) + N(\alpha_{\text{in}} \mathbf{c}_{\text{in}}(t) - \alpha_e \mathbf{c}) \right] \quad (29)$$

$$\mathbf{c}(t=0) = \mathbf{c}_0 \quad (30)$$

where α_{in} is a diagonal matrix of fractional inlet flow rates into cells, α_e is a matrix of fractional auxiliary flow rates, $\mathbf{r}(\mathbf{c})$ is a vector of dimensionless reaction rates, and the dimensionless discrete convection (loop) operator \mathbf{A} is given by

$$\mathbf{A} = N \begin{pmatrix} 1 & 0 & \dots & 0 & -1 \\ -1 & 1 & \dots & 0 & 0 \\ 0 & -1 & \dots & 0 & 0 \\ \vdots & \vdots & \ddots & \vdots & \vdots \\ 0 & 0 & \dots & -1 & 1 \end{pmatrix} \quad (31)$$

[Remark: The discrete loop operator can be obtained from the continuum case by replacing the derivative $\frac{\partial c}{\partial x}$ by the first-order upwind difference $\frac{c_j - c_{j-1}}{\Delta x} = N(c_j - c_{j-1})$ and

noting $c_0 = c_N$]. It is easily seen that the characteristic equation for the eigenvalue problem

$$\mathbf{A}\mathbf{y} = -\lambda\mathbf{y} \quad (32)$$

can be expressed as

$$h_d(\lambda) \equiv \left(1 + \frac{\lambda}{N}\right)^N - 1 = 0 \quad (33)$$

and the spectrum can be expressed as

$$\lambda_m = -N \left[1 - \cos\left(\frac{2\pi m}{N}\right) \right] + iN \sin\left(\frac{2\pi m}{N}\right) \quad (34)$$

$$= -N[1 - \omega^m]; \quad m = 0, 1, \dots, N-1 \quad (35)$$

where ω is the N th root of unity given by $e^{2\pi i/N}$. Thus, for odd N , there is one zero eigenvalue while all others are complex, while for even N , all eigenvalues except two are complex. We also note that the spectrum of the discrete convective loop approaches that of the continuous case in the limit $N \rightarrow \infty$, but the approach (or convergence) is not uniform. As in the continuum case, the discrete convection operator \mathbf{A} is not symmetric with respect to the usual inner product in $\mathbb{R}^N/\mathbb{C}^N$

$$\langle \mathbf{y}, \mathbf{v} \rangle = \sum_{j=1}^N y_j \bar{v}_j. \quad (36)$$

(Here, the overbar denotes the complex conjugate.) The adjoint operator ($\mathbf{A}^* = \mathbf{A}^T$) here corresponds to a discrete convective loop in the clockwise direction. The eigenvector corresponding to the zero eigenvalue is the uniform vector \mathbf{y}_0 with $\mathbf{y}_0^T = (1, 1, \dots, 1)$. We take the corresponding adjoint (or left) eigenvector as $\mathbf{v}_0^T = \frac{1}{N}(1, 1, \dots, 1)$, so that the inner product of \mathbf{y}_0 and \mathbf{v}_0 is unity. Defining the average concentration in the discrete loop as

$$\langle c \rangle(t) = \langle \mathbf{c}, \mathbf{v}_0 \rangle = \frac{1}{N} \sum_{j=1}^N c_j \quad (37)$$

the above model may be reduced to the classical ideal CSTR model given by Eqs. 23 and 24 in the limit of $\epsilon \rightarrow 0$. Taking the dot product of Eq. 29 with \mathbf{v}_0 and noting that

$$c_m^{\text{in}}(t) = N \mathbf{v}_0^T \boldsymbol{\alpha}_{\text{in}} \mathbf{c}_{\text{in}}(t) = \sum_{j=1}^N \alpha_{j,\text{in}} c_{j,\text{in}}(t) \quad (38)$$

$$N \mathbf{v}_0^T \boldsymbol{\alpha}_e \mathbf{c} = N \mathbf{v}_0^T \boldsymbol{\alpha}_e \mathbf{y}_0 \langle c \rangle = \langle c \rangle \quad (\text{for } \epsilon \rightarrow 0) \quad (39)$$

we obtain the zeroth-order model given by Eq. 23. However, for small but finite ϵ , mixing effects become important as shown in the next section.

The convection-diffusion operator

So far, we have considered only the convection dominated case and ignored diffusional effects along the loop. Although our focus in the next section is the practical convection dominated case, we consider here briefly the effect of axial diffusion and how the spectrum of the convection operator changes with the addition of axial diffusion. We start again with the continuous case for which the convection-diffusion operator is given by

$$\mathcal{L}_{\text{CD}} \equiv -D_e \frac{d^2 C}{dx'^2} + \langle u \rangle \frac{dC}{dx'}; \quad 0 < x' < L$$

with periodic boundary conditions. Here, D_e is the effective axial diffusivity of the reactant, and $\langle u \rangle$ is the average velocity in the loop. After casting the model in dimensionless form, the relevant eigenvalue problem may be expressed as

$$-\frac{1}{Pe} \frac{d^2 w}{dx^2} + \frac{dw}{dx} = \lambda w, \quad 0 < x < 1; \quad (40)$$

$$w(0) = w(1), \quad w'(0) = w'(1)$$

where Pe is the Peclet number based on the loop length ($Pe = \frac{\langle u \rangle L}{D_e}$). We note that the Peclet number takes large values for the case of loop or recycle reactors and hence only the case of $Pe \gg 1$ is of interest here. After some algebra, it may be shown that the eigenvalues (for any $Pe > 0$) are given by

$$\lambda_m = -\frac{4m^2\pi^2}{Pe} - 2m\pi i; \quad m = 0, \pm 1, \pm 2, \dots \quad (41)$$

Thus, the zero eigenvalue persists for finite values of the Peclet number, but all other eigenvalues appear in complex conjugate pairs with the real part approaching zero as $Pe \rightarrow \infty$.

We want to see if a similar relation can be found for the discrete case. Here, the analog of diffusion is the superposition of equal amounts of forward and backward flow (q_D) on the main convective flow (Q_R). However, to compare the discrete and continuous cases on an equal footing, we must match the characteristic times properly. For example, as the convection or loop time for the case of N discrete cells is proportional to N , the diffusion time should be proportional to N^2 . This fact can be easily missed if one is working with the volumetric flow rates for the main flow in the loop (convective) and backmixing (diffusive) without thinking of them as analogs of convection and diffusion, respectively. The loop time or convection time may be expressed as $t_c = \frac{NA_c \Delta x}{q_R}$ where A_c is the cross-sectional area and $V_c = A_c \Delta x$ is volume of one cell, hence making $NA_c \Delta x$ the total volume of the reactor. To obtain the characteristic diffusion time, one needs the analog of diffusivity here. As q_D/A_c is the diffusive velocity, it should be linearly proportional to $D/\Delta x$. Then, $t_{\text{diff}} = (N\Delta x)^2/(q_D \Delta x/A_c) = N^2 A_c \Delta x/q_D$. Hence, for the discrete loop, the Peclet number can be written as $p = t_{\text{diff}}/t_c = NQ_R/q_D$. With this nondimensionalization, the discrete convection-diffusion operator may be expressed as

$$\mathbf{A}_{cd} = N \begin{pmatrix} \left(\frac{2N}{p} + 1\right) & -\frac{N}{p} & \dots & \dots & 0 & -\left(1 + \frac{N}{p}\right) \\ -\left(1 + \frac{N}{p}\right) & \left(\frac{2N}{p} + 1\right) & \dots & \dots & 0 & 0 \\ \vdots & \vdots & \ddots & \ddots & \vdots & \vdots \\ 0 & 0 & \dots & \dots & \left(\frac{2N}{p} + 1\right) & -\frac{N}{p} \\ -\frac{N}{p} & 0 & \dots & \dots & -\left(1 + \frac{N}{p}\right) & \left(\frac{2N}{p} + 1\right) \end{pmatrix} \quad (42)$$

The matrix \mathbf{A}_{cd} is clearly circulant, and it is this matrix whose eigenvalues should correspond to those of the operator in the continuum version. Using the theory of discrete Fourier transform for circulant matrices,⁷ it can be shown that the eigenvalues of the above matrix are given by

$$\lambda_m = -N \left(\frac{2N}{p} + 1 \right) + \frac{N^2}{p} \left[\exp \left(\frac{2\pi m i}{N} \right) \right] + \left(N + \frac{N^2}{p} \right) \left[\exp \left(\frac{2\pi m i}{N} \right) \right] = -N(1 - \omega^m) - \frac{4N^2}{p} \sin^2 \left(\frac{\pi m}{N} \right);$$

$$m = 0, 1, \dots, N-1 \quad (43)$$

Again, for odd N , there is one zero eigenvalue while all others are complex while for even N , all eigenvalues except two are complex. As $p \rightarrow \infty$, the spectrum approaches that of the discrete convection operator, Eq. 35, while for $N \rightarrow \infty$, it approaches that of the continuum case.

Before closing this section, it should be pointed out that the spectrum of both the discrete and the continuous convection and convection-diffusion operators with the loop (or recycle) boundary condition is fundamentally different from that of the same operators with other types of boundary conditions. For example, the traditional continuous convection-diffusion operator with Danckwerts' boundary conditions (and no recycle) leads to the eigenvalue problem

$$-\frac{1}{Pe} \frac{d^2 w}{dx^2} + \frac{dw}{dx} = \lambda w, \quad 0 < x < 1;$$

$$-\frac{1}{Pe} \frac{dw}{dx}(0) + w(0) = 0, \quad w'(1) = 0 \quad (44)$$

Here, the spectrum is real and discrete for any finite value of Pe , and only in the limit of $Pe \rightarrow \infty$ (plug flow limit) does it become continuous. The same is true for the discrete (cell) model of the convection-diffusion operator without recycle. Thus, the loop/recycle boundary condition is essential for the existence of zero eigenvalue as well as other complex eigenvalues.

Low-Dimensional Description of Loop and Recycle Reactors with Finite Mixing Effects

We now wish to exploit our knowledge of spectral properties studied earlier to derive low-dimensional models describing the loop and recycle reactors using the Liapunov-Schmidt (LS) procedure.

Discrete models

We consider again a discrete system of N interacting cells arranged in a loop and in which the flow is convection dominated. As discussed earlier, the vector balance equation for any species is given by

$$\mathbf{A}\mathbf{c} = \epsilon \left[-\frac{d\mathbf{c}}{dt} - \mathbf{D}\mathbf{a}(\mathbf{c}) + N\{\boldsymbol{\alpha}_{in}\mathbf{c}_{in}(t) - \boldsymbol{\alpha}_e\mathbf{c}\} \right] \quad (45)$$

and reduces to the classical ideal CSTR model given by Eq. 23 in the limit of $\epsilon \rightarrow 0$. Here, the objective is to consider the practical case of small but finite ϵ and reduce the number of degrees of freedom in the system. In practice, the quantity of interest is the exit (mixing-cup or flow weighted) concentration. Thus, in addition to reducing the degrees of freedom,

we would like to express the reduced order model directly in terms of this and other concentration modes that are of interest. [Note: To reduce the number of indices, we have not used a species index. As shown later, the generalization of the averaged model to include an arbitrary number of species and reactions is straightforward].

As the averaging of continuous and discrete models using the LS procedure is explained in detail elsewhere,⁹⁻¹² we outline only some intermediate steps here. We expand the concentration vector as

$$\mathbf{c} = \langle \mathbf{c} \rangle \mathbf{y}_0 + \mathbf{c}' \quad (46)$$

and take the inner product of Eq. 45 with the adjoint eigenvector \mathbf{v}_0 to obtain the averaged or global equation

$$\frac{d\langle \mathbf{c} \rangle}{dt} + \mathbf{D}\mathbf{a}(\langle \mathbf{r}(\mathbf{c}) \rangle) - \mathbf{c}_m^{\text{in}}(t) + \mathbf{c}_m = 0 \quad (47)$$

Here, $\mathbf{c}_m^{\text{in}}(t)$ and \mathbf{c}_m are the inlet and exit cup-mixing (flow weighted) concentrations of the species, respectively. These are defined as

$$\mathbf{c}_m^{\text{in}}(t) = N\mathbf{v}_0^T \boldsymbol{\alpha}_{in} \mathbf{c}_{in}(t) = \sum_{j=1}^N \alpha_{j,in} c_{j,in}(t) \quad (48)$$

$$\mathbf{c}_m = N\mathbf{v}_0^T \boldsymbol{\alpha}_e \mathbf{c} \quad (49)$$

[Remark: When there is a single exit stream from cell m , $N\mathbf{v}_0^T \boldsymbol{\alpha}_e$ is a row vector having unity in the m th position and zeros in all other positions. In the more general case, $N\mathbf{v}_0^T \boldsymbol{\alpha}_e \mathbf{c}$ is a flow weighted average concentration]. Now, the nonlinear reaction rate term may be simplified as

$$\begin{aligned} \langle \mathbf{r}(\mathbf{c}) \rangle &= \frac{1}{N} \sum_{j=1}^N r(\langle \mathbf{c} \rangle + \mathbf{c}'_j) \\ &= r(\langle \mathbf{c} \rangle) + \frac{dr}{dc}(\langle \mathbf{c} \rangle) \frac{1}{N} \sum_{j=1}^N \mathbf{c}'_j + O(|\mathbf{c}'|^2) \\ &= r(\langle \mathbf{c} \rangle) + O(|\mathbf{c}'|^2) \end{aligned} \quad (50)$$

The last equality follows from the definition of average and our choice of complementary spaces (see Figure 2). Specifically, taking inner product of Eq. 46 with \mathbf{v}_0 gives

$$\langle \mathbf{c}', \mathbf{v}_0 \rangle = \mathbf{v}_0^T \mathbf{c}' = \frac{1}{N} \sum_{j=1}^N \mathbf{c}'_j = 0 \quad (51)$$

The relation expressed by Eq. 50 is crucial, as it shows that the volume-averaged reaction rate is equal to the reaction rate at the volume-averaged concentration, with an error that is proportional to ϵ^2 . Another important point to note is that the source term (reaction rate) is evaluated at the volume-averaged concentration $\langle \mathbf{c} \rangle$, while the quantity of interest is the flow weighted exit concentration \mathbf{c}_m . The closure of the model is obtained by relating the two concentration modes, $\langle \mathbf{c} \rangle$ and \mathbf{c}_m . We obtain this relation here only to leading order in ϵ by expanding \mathbf{c}' as

$$\mathbf{c}' = \epsilon \mathbf{c}_1 + O(\epsilon^2) \quad (52)$$

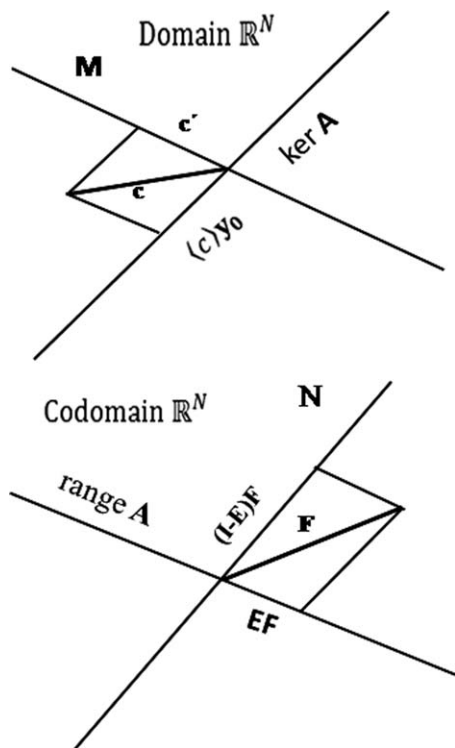


Figure 2. A schematic diagram of the subspaces used in the finite-dimensional version of the LS reduction.

Substituting this into Eq. 45, we get a linear inhomogeneous equation for \mathbf{c}_1

$$\mathbf{A}\mathbf{c}_1 = -\mathbf{y}_0 \left(\frac{d\langle c \rangle}{dt} + \text{Dar}(\langle c \rangle) \right) + N \{ \boldsymbol{\alpha}_{\text{in}} \mathbf{c}_{\text{in}}(t) - \langle c \rangle \boldsymbol{\alpha}_{\text{e}} \mathbf{y}_0 \} \quad (53)$$

Now, from the global equation 47, we find that at the zeroth-order

$$\frac{d\langle c \rangle}{dt} + \text{Dar}(\langle c \rangle) = c_{\text{m}}^{\text{in}}(t) - \langle c \rangle \quad (54)$$

We use this in Eq. 53 to get

$$\mathbf{A}\mathbf{c}_1 = [N\boldsymbol{\alpha}_{\text{in}} \mathbf{c}_{\text{in}}(t) - \mathbf{y}_0 c_{\text{m}}^{\text{in}}(t)] - \langle c \rangle (N\boldsymbol{\alpha}_{\text{e}} - \mathbf{I})\mathbf{y}_0 \quad (55)$$

which must be solved with the constraint on \mathbf{c}_1 given by

$$\mathbf{v}_0^T \mathbf{c}_1 = 0 \quad (56)$$

It can be observed that the solution of (55) is unique as the solvability condition is satisfied (as $N\mathbf{v}_0^T \boldsymbol{\alpha}_{\text{e}} \mathbf{y}_0 = 1$). To close the global equation 47, we premultiply the equation

$$\mathbf{c} = \langle c \rangle \mathbf{y}_0 + \epsilon \mathbf{c}_1 + O(\epsilon^2) \quad (57)$$

by $N\mathbf{v}_0^T \boldsymbol{\alpha}_{\text{e}}$ to obtain the relationship between the two concentration modes as

$$c_{\text{m}} = \langle c \rangle + \delta_{\text{mix},2} c_{\text{m}}^{\text{in}}(t) - \delta_{\text{mix},1} \langle c \rangle + O(\epsilon^2) \quad (58)$$

where $\delta_{\text{mix},2}$ and $\delta_{\text{mix},1}$ are the two mixing coefficients defined as follows

$$\delta_{\text{mix},1} = \epsilon N \mathbf{v}_0^T \boldsymbol{\alpha}_{\text{e}} \mathbf{z}_1 \quad (59)$$

$$\mathbf{A}\mathbf{z}_1 = (N\boldsymbol{\alpha}_{\text{e}} - \mathbf{I})\mathbf{y}_0; \langle \mathbf{z}_1, \mathbf{v}_0 \rangle = 0 \quad (60)$$

and

$$\delta_{\text{mix},2} = \epsilon N \mathbf{v}_0^T \boldsymbol{\alpha}_{\text{e}} \mathbf{z}_2 \quad (61)$$

$$\mathbf{A}\mathbf{z}_2 = \left(N\boldsymbol{\alpha}_{\text{in}} \frac{\mathbf{c}_{\text{in}}(t)}{c_{\text{m}}^{\text{in}}(t)} - \mathbf{y}_0 \right); \langle \mathbf{z}_2, \mathbf{v}_0 \rangle = 0 \quad (62)$$

We note that the first mixing coefficient depends only on the various auxiliary flow rates (and the connectivity between various cells) and is independent of the inlet reactant concentrations. The second mixing coefficient depends on both the auxiliary flow rates and the inlet reactant concentrations and, hence, can be a function of time. As explained elsewhere,¹¹ it is convenient to regularize the local Eq. 58 by replacing $\langle c \rangle$ in the third term on the r.h.s. of Eq. 58 by c_{m} . This does not change the accuracy of the reduced order model but increases its range of validity. To summarize, the two-mode reduced order model is given by

$$\frac{d\langle c \rangle}{dt} = c_{\text{m}}^{\text{in}}(t) - c_{\text{m}} - \text{Dar}(\langle c \rangle) + O(\epsilon^2) \quad (63)$$

$$c_{\text{m}} = \langle c \rangle + \delta_{\text{mix},2}(t) c_{\text{m}}^{\text{in}}(t) - \delta_{\text{mix},1} c_{\text{m}} + O(\epsilon^2) \quad (64)$$

We note that this “two-mode two-mixing coefficient differential-algebraic equation model” reduces to the classical ideal CSTR model in the limit of $\epsilon \rightarrow 0$ while for small but finite ϵ , it retains all the main qualitative and quantitative features of the full model. [Remark: The cup-mixing concentration c_{m} can be eliminated from the above model to obtain a single equation for $\langle c \rangle$. While this simplifies the transient analysis of the model, as stated earlier, the (measured) quantity of practical interest is c_{m} . Thus, we still have a two-mode model with c_{m} fully slaved to $\langle c \rangle$.]

The above reduced order model can be easily generalized to the case of R reactions among S species

$$\sum_{j=1}^S v_{ij} A_j = 0; i = 1, 2, \dots, R \quad (65)$$

Assuming a constant density system, the reduced order model in dimensional form can be expressed as

$$\frac{d\langle C_j \rangle}{dt'} = \frac{C_{\text{m},j}^{\text{in}}(t') - C_{\text{m},j}}{\tau} + \sum_{i=1}^R v_{ij} r_i(\langle C_1 \rangle, \langle C_2 \rangle, \dots, \langle C_S \rangle) \quad (66)$$

$$C_{\text{m},j} = \langle C_j \rangle + \delta_{\text{mix},2,j} C_{\text{m},j}^{\text{in}}(t') - \delta_{\text{mix},1,j} C_{\text{m},j}; j = 1, 2, \dots, S \quad (67)$$

$$\delta_{\text{mix},2,j} = \epsilon N \mathbf{v}_0^T \boldsymbol{\alpha}_{\text{e}} \mathbf{z}_{2j} \quad (68)$$

$$\mathbf{A}\mathbf{z}_{2j} = \left(N\boldsymbol{\alpha}_{\text{in}} \frac{\mathbf{C}_{\text{in},j}(t')}{C_{\text{m},j}^{\text{in}}(t')} - \mathbf{y}_0 \right); \langle \mathbf{z}_{2j}, \mathbf{v}_0 \rangle = 0 \quad (69)$$

where τ is the space time and $\delta_{\text{mix},1,j}$ (which is the same for all species) is given by Eqs. 59 and 60. We also note that if any reactant (or intermediate) species is not present in the inlet streams, then $\delta_{\text{mix},2,j}$ is zero for that species.

We present explicit expressions for the mixing coefficients as well as illustrate the application of the reduced order models to nonlinear kinetics in the next section.

Continuum models

We now consider the development of reduced order models for loop and recycle reactors, starting with the loop reactor case.

Loop Reactors. We consider the loop reactor model with two inlets but a single outlet. In general, such a system would be characterized by mixing and complicated hydrodynamics at the entry points. The starting model considered here circumvents that issue by using the fact that for all practical purposes, the loop flow rate is much larger than the auxiliary feed flow rates obviating the need to concentrate on hydrodynamic matters. Also, our starting model is convection dominated, namely, a first-order nonlinear partial differential equation of the form given by Eq. 11. Unlike some other models where it is assumed that the entry points are finite volume CSTRs, we take the inlet and outlets to be of zero volume for simplicity. Also, we consider just two inlets and a single outlet for the purpose of illustration, noting that it can be readily extended to more general arrangements. We want to exploit the spectral properties outlined in the previous section to get low-dimensional models, which can describe mixing effects in the reactor up to first order in the small parameter (ratio of feed to recycle flow rates). We note that at the larger reactor scale, mixing occurs due to circulation, while the smaller inlet flows provide means for additional mixing and hence add in detail to the model. We denote the entering flow rates are q_{F_i} and the corresponding feed concentrations $c_{F_i}(t)$ and define $q_F = q_{F_1} + q_{F_2}$, $\alpha_i = q_{F_i}/q_F$ and $c_m^{\text{in}}(t) = \sum_{i=1}^2 \alpha_i c_{F_i}(t)$. Let the domain be marked with special points θ_i where the inlets/outlet are, for example, the first inlet is at θ_1 . The flow rates undergo jumps at these points, and we have three distinct flow rates that are given as Q_R between $\theta = 0$ (exit, same as $\theta = 1$) and θ_1 , $Q_R + q_{F_1}$ between θ_1 and θ_2 , and $Q_R + q_{F_1} + q_{F_2}$ between θ_2 and 1. We would then have the governing equation

$$\frac{\partial c}{\partial x} = -\epsilon \left[\text{Dar}(c) + \frac{\partial c}{\partial t} + k(x) \frac{\partial c}{\partial x} \right]; \quad (70)$$

$$x \in (0, \theta_1) \cup (\theta_1, \theta_2) \cup (\theta_2, 1), \quad t > 0$$

Here, $k(x)$ is given by the discontinuous function

$$k(x) = \begin{cases} 0, & 0 < x < \theta_1 \\ \alpha_1, & \theta_1 < x < \theta_2 \\ 1, & \theta_2 < x < 1 \end{cases} \quad (71)$$

and arises because of the velocity jumps (that are of order ϵ) in our model. Also, at each entry point, we get a species balance

$$q_{F_1} c_{F_1}(t) + Q_R c(\theta_1^-) = (Q_R + q_{F_1}) c(\theta_1^+) \quad (72)$$

$$q_{F_2} c_{F_2}(t) + (Q_R + q_{F_1}) c(\theta_2^-) = (Q_R + q_{F_1} + q_{F_2}) c(\theta_2^+) \quad (73)$$

On division by Q_R we can write them as

$$c(\theta_1^+) - c(\theta_1^-) = \epsilon [\alpha_1 c_{F_1}(t) - \alpha_1 c(\theta_1^+)] \quad (74)$$

$$c(\theta_2^+) - c(\theta_2^-) = \epsilon [\alpha_2 c_{F_2}(t) + \alpha_1 c(\theta_2^-) - c(\theta_2^+)] \quad (75)$$

These serve as the boundary conditions (and become requirements of continuity of concentration when $\epsilon \rightarrow 0$).

As noted in the previous section, a zero eigenvalue exists in the limit of $\epsilon \rightarrow 0$ and the corresponding eigenfunction can be normalized to 1. Let us call this eigenfunction ψ_0 . These are all the ingredients needed to effect the dimension reduction. We can now start applying the LS averaging procedure to the model with the anticipation that it would lead to a two mixing coefficients model as in the discrete case.

The averaged (global) equation can be obtained by taking an inner product of Eq. 70 with ψ_0

$$\begin{aligned} & c(1^-) - c(\theta_2^+) + c(\theta_2^-) - c(\theta_1^+) + c(\theta_1^-) - c(0^+) \\ &= \epsilon \left[-\text{Da} \langle r(c) \rangle - \frac{d \langle c \rangle}{dt} \right] \\ &+ \epsilon [\alpha_1 (c(\theta_2^-) - c(\theta_1^+)) + c(1^-) - c(\theta_2^+)] \end{aligned} \quad (76)$$

We can simplify this using the boundary conditions (74) and (75) and noting that

$$\langle r(c) \rangle = r(\langle c \rangle) + O(\epsilon^2) \quad (77)$$

$$c(0) = c_m \quad (78)$$

to obtain the global equation in the standard form

$$\frac{d \langle c \rangle}{dt} = c_m^{\text{in}}(t) - c_m - \text{Da} r(\langle c \rangle) + O(\epsilon^2) \quad (79)$$

If we compare this equation to Eq. 47 of the discrete case, we can see that it is basically the same equation (which is to be anticipated). Now, as in the discrete case, we write $c = \langle c \rangle + c'$ with $c' = \epsilon c_1 + O(\epsilon^2)$, and substitute in Eq. 70, to get the local equation

$$\frac{\partial c_1}{\partial x} = -\text{Da} r(\langle c \rangle) - \frac{d \langle c \rangle}{dt} \quad (80)$$

$$= \langle c \rangle - c_m^{\text{in}}(t) \quad (81)$$

Upon integration, this gives

$$c_1(x, t) = (\langle c \rangle - c_m^{\text{in}}(t))x + S_i \quad (82)$$

where S_i is an integration constant. The reason we have used the index i in S_i is because it is not expected to be a constant in the whole domain but have jumps and be a constant between any two inlets/outlets. We call the constant for the domain between $\theta = 0$ to $\theta = \theta_1$ as S_1 , and the next constants S_2 and S_3 in the domains between $\theta = \theta_1$ to $\theta = \theta_2$ and $\theta = \theta_2$ to $\theta = 1$, respectively. These can be evaluated by using the constraint $\langle c_1, \psi_0 \rangle = 0$ and the boundary conditions

$$\alpha_1 (\langle c \rangle - c_{F_1}(t)) = c_1(\theta_1^-) - c_1(\theta_1^+) \quad (83)$$

$$\alpha_2 (\langle c \rangle - c_{F_2}(t)) = c_1(\theta_2^-) - c_1(\theta_2^+) \quad (84)$$

along with the loop boundary condition

$$c_1(1^-) = c_1(0^+) \quad (85)$$

This leads to the following system of three linear equations for S_i (but with only 2 being independent):

$$S_i - S_{i+1} = \alpha_i (\langle c \rangle - c_{F_i}(t)), \quad i = 1, 2 \quad (86)$$

and

$$S_3 - S_1 = -(\langle c \rangle - c_m^{\text{in}}(t)) \quad (87)$$

This is a circulant system for S_i with the corresponding matrix representation of the system echoing the discrete convection operator. In this simple case, it can be solved explicitly as

$$\begin{aligned} S_2 &= S_1 - \alpha_1(\langle c \rangle - c_{F_1}(t)) \\ S_3 &= S_2 - \alpha_2(\langle c \rangle - c_{F_2}(t)) = S_1 - \alpha_1(\langle c \rangle - c_{F_1}(t)) - \alpha_2(\langle c \rangle - c_{F_2}(t)) \\ S_1 &= \alpha_1(\langle c \rangle - c_{F_1}(t))(1 - \theta_1) + \alpha_2(\langle c \rangle - c_{F_2}(t))(1 - \theta_2) \\ &\quad - \frac{1}{2}(\langle c \rangle - c_m^{\text{in}}(t)) \end{aligned}$$

Thus, the local equation may be expressed as

$$\begin{aligned} c(0, t) &= \langle c \rangle + \epsilon c_1(0, t) + O(\epsilon^2) \\ &= \langle c \rangle + \epsilon S_1 + O(\epsilon^2) \\ &= \langle c \rangle + \delta_{\text{mix}, 2}(t) c_m^{\text{in}}(t) - \delta_{\text{mix}, 1} c_m + O(\epsilon^2) \end{aligned} \quad (88)$$

with the mixing coefficients given by

$$\delta_{\text{mix}, 2} = \epsilon \left[\frac{1}{2} - \sum_{i=1}^2 \alpha_i (1 - \theta_i) \frac{c_{F_i}(t)}{c_m^{\text{in}}(t)} \right] \quad (89)$$

$$\delta_{\text{mix}, 1} = \epsilon \left[\frac{1}{2} - \sum_{i=1}^2 \alpha_i (1 - \theta_i) \right] \quad (90)$$

To summarize, the reduced order model is the same for both the discrete and the continuum convection operators with only a slight difference in the formulas for the mixing coefficients. We also note that the generalization of the above formulas for the mixing coefficients to any number of entering streams is straightforward. We now consider recycle reactors as a special case.

Recycle Reactors. The difference between loop and recycle reactors appears in the simplification of the boundary condition. Thus, the global equation remains unchanged but the local equation simplifies to

$$c_m = c(1, t) = \langle c \rangle + \frac{\epsilon}{2}(\langle c \rangle - c_m^{\text{in}}(t)) + O(\epsilon^2) \quad (91)$$

and the two mixing coefficients are given by

$$\delta_{\text{mix}, 1} = \delta_{\text{mix}, 2} = -\frac{\epsilon}{2} \quad (92)$$

In this special case, we can substitute Eq. 91 and rescale the time and Damköhler number

$$\hat{t} = t \left(1 + \frac{\epsilon}{2} \right) \quad \hat{Da} = \frac{Da}{\left(1 + \frac{\epsilon}{2} \right)} \quad (93)$$

to express the global equation in the same form as that of the zeroth-order (CSTR) model, that is

$$\frac{d\langle c \rangle}{d\hat{t}} = c_m^{\text{in}}(t) - \langle c \rangle - \hat{Da}r(\langle c \rangle) + O(\epsilon^2) \quad (94)$$

Thus, for the special case of a recycle reactor, the reduced order model to first order in ϵ can be scaled to the zeroth-order CSTR model in terms of the average concentration

$(\langle c \rangle)$, with the exit or cup-mixing concentration (c_m) slaved to $\langle c \rangle$ by Eq. 91.

Convergence and accuracy of reduced order models

It should be stressed again that the above simplification of the full discrete and continuous convection models by the LS reduction is only valid in the limit of small ϵ . To determine the exact range of validity and accuracy of the first-order truncated model, we need to continue the averaging procedure to higher orders in ϵ and examine the convergence and accuracy of the perturbation series. As the continuation of the perturbation series to higher orders is straightforward and has been discussed elsewhere for other problems,¹⁰ we comment here only on the convergence and accuracy of the truncated models.

First, we recall that the assumption of $\epsilon \ll 1$ implies that the loop circulation time (or macromixing time) is much smaller compared to the convection or residence time. Another implicit assumption is that the loop circulation time is the smallest time scale in the system. Equivalently, this means all other parameters representing the ratios of other time scales of the system are assumed to be order unity. For example, it was assumed that the Damköhler number (ratio of convection to reaction time scales) is of order unity. Based on this assumption, we expect the reduced order model to be valid when ϵDa (which represents the ratio of circulation time to reaction time) is of order unity or smaller. Thus, the perturbation series may not converge if $\epsilon Da \gg 1$. With respect to the accuracy of the truncated model, we note that when Da is of order unity, the error is of $O(\epsilon^2)$ while it is of order ϵ when ϵDa is of order unity. These intuitive estimates (or conjectures) can be verified for specific reaction kinetics and cell (or loop) arrangements. For example, for the case of linear kinetics in a two cell arrangement (with reactants and products entering and leaving the same cell), it may be shown that the exact local equation is of the form

$$c' = \frac{\delta_1 Da}{1 + \delta_1 Da} \langle c \rangle; \quad \delta_1 = \frac{\epsilon}{4} \quad (95)$$

and the perturbation series converges absolutely provided $\delta_1 Da < 1$. For this case, the difference between the exact exit concentration (c_E) and that predicted by the reduced order model (c_{LD}) may be expressed as

$$c_E - c_{LD} = \frac{\epsilon^2 Da^3}{16(1 + Da)^2} \quad (96)$$

We expect that the above estimates on the range of convergence and accuracy of the truncated reduced order models to be also valid for the case of multiple reactions provided the Damköhler number is defined based on the smallest reaction time scale.

Application of Averaged Models

In this section, we illustrate the application of the reduced order models to examine the impact of mixing effects on the conversion, yield, and selectivity for the case of isothermal nonlinear kinetics. Before considering specific examples, we examine first the dependence of the two mixing coefficients on the flow rates and entry points of various feed streams and inlet concentrations of reactants.

Evaluation of mixing coefficients

We consider first the discrete case with a premixed feed entering the first cell. If the product stream also leaves from the same cell, it may be shown from Eqs. 59–62 that

$$\delta_{\text{mix},1} = \delta_{\text{mix},2} = \epsilon \left(\frac{N-1}{2N} \right) \quad (97)$$

Thus, except for the case of $N = 1$ (ideal CSTR), both the mixing coefficients for this special case are always positive and equal for all the species that are present in the feed stream. As stated earlier, for any intermediate species, the second mixing coefficient is zero. We note that for large N , the mixing coefficients approach the continuum limit of $\frac{\epsilon}{2}$.

The second discrete scenario we consider is that of a premixed feed entering the first cell and a single product stream leaving cell m ($1 \leq m \leq N$). We can obtain the mixing coefficients by solving Eqs. 59–62 (see Appendix B)

$$\delta_{\text{mix},1} = \delta_{\text{mix},2} = \epsilon \left(\frac{N-2m+1}{2N} \right) \quad (98)$$

Thus, in this case, the mixing coefficients can be either positive (e.g., $m = 1$) or negative (e.g., $m = N$) and for large N , vary between the continuum limits of $-\frac{\epsilon}{2}$ and $\frac{\epsilon}{2}$.

As the final discrete situation, we consider more general reactor arrangements with multiple entrances and a single exit while each feed stream has one or more species. As the aim of this work is to illustrate how the low-dimensional models presented here capture the effects of finite mixing, we study only two-cell systems for simplicity. Three distinct two-cell arrangements are possible for a system with two reactants A and B (see Figure 3). The first one corresponds to both A and B entering in cell 1 and product leaving in cell 2 (as shown in the top diagram of Figure 3). In this case, as discussed earlier, the mixing coefficients for both A and B are equal and negative regardless of relative dilutions ($\delta_{\text{mix},1} = \delta_{\text{mix},2A} = \delta_{\text{mix},2B} = -\frac{\epsilon}{4}$). The second case corresponds to the situation where both A and B enter cell 1 and the product also leaves cell 1. Again, as discussed earlier, the mixing coefficients for this case are equal and positive ($\delta_{\text{mix},1} = \delta_{\text{mix},2A} = \delta_{\text{mix},2B} = \frac{\epsilon}{4}$). The third case corresponds to both A and B entering in different cells (as shown in the bottom diagram of Figure 3). For this situation, the mixing coefficients can be calculated to be

$$\delta_{\text{mix},1} = \frac{\epsilon}{4} (1 - 2\alpha_1) \quad (99)$$

$$\delta_{\text{mix},2j} = \frac{\epsilon}{4} \left(\frac{\alpha_2 c_{2,j}^{\text{in}} - \alpha_1 c_{1,j}^{\text{in}}}{\alpha_1 c_{2,j}^{\text{in}} + \alpha_2 c_{1,j}^{\text{in}}} \right); \quad j = A, B \quad (100)$$

Here, α_i is the fractional inlet flow rate into cell i and $c_{i,j}^{\text{in}}$ is the concentration of species j ($j = A, B$) in the inlet stream to cell i ($i = 1, 2$). As noted in the previous section, the first mixing coefficient is the same for all species, whereas the second one is zero for any intermediate species. Also, the effect of relative dilution of streams and inlet concentrations on mixing coefficients can be felt only in the third arrangement.

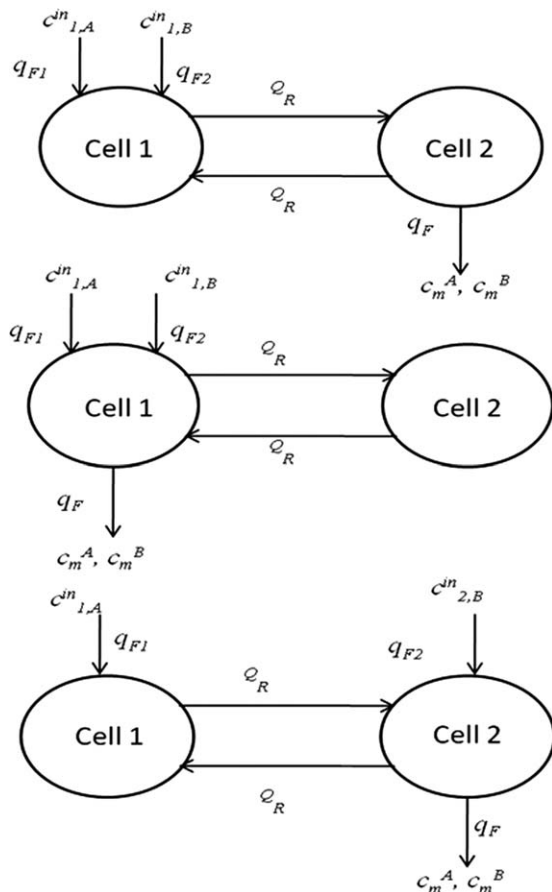


Figure 3. Schematic diagrams illustrating how the reactant entrance and product exit locations influence the mixing coefficients in two-cell arrangements.

Next, we consider different continuum models. For the case of a single feed and exit stream, an easy calculation shows that

$$\delta_{\text{mix},1} = \delta_{\text{mix},2} = \epsilon \left[\frac{1}{2} - (1 - \theta_1) \right] \quad (101)$$

We note that the two limiting cases of $\theta_1 = 0$ and $\theta_1 = 1$ correspond to the case of recycle reactor (for which both mixing coefficients are negative) and loop reactor (for which both mixing coefficients are positive). For the general case of M entrances and a single exit stream, from the development in the previous section, it is easily seen that

$$\delta_{\text{mix},2j} = \epsilon \left[\frac{1}{2} - \sum_{i=1}^M \alpha_i (1 - \theta_i) \frac{c_{i,j}^{\text{in}}(t)}{c_{m,j}^{\text{in}}(t)} \right]; \quad c_{m,j}^{\text{in}}(t) = \sum_{i=1}^M \alpha_i c_{i,j}^{\text{in}}(t) \quad (102)$$

$$\delta_{\text{mix},1} = \epsilon \left[\frac{1}{2} - \sum_{i=1}^M \alpha_i (1 - \theta_i) \right] \quad (103)$$

From the above discussion, it is clear that the mixing coefficients can be positive, negative, or zero depending on the relative flow rates and entrance and exit points of various auxiliary streams and inlet concentrations of the reactants. While the zeroth-order CSTR model (with $\delta_{\text{mix},1} = \delta_{\text{mix},2} =$

0) ignores all the details about entrance and exit locations and relative concentrations and flow rates of various streams, the two-mode first-order model includes all this information through the mixing coefficients. Thus, the two-mode models extend the ideal CSTR model to accommodate the effects of finite mixing.

Examples

We now illustrate the impact of mixing effects on the conversion, yield, and selectivity for the case of single and multiple reactions (*Remark:* In the examples below, $\delta_{\text{mix},1} = \delta_1$ and $\delta_{\text{mix},2,j} = \delta_{2j}$).

The first example we consider is that of a single one step reaction $A \rightarrow P$ with the rate of disappearance of A given by $r = kR(C_A)$. The goal here is to determine the sensitivity of the steady-state conversion predicted by the ideal CSTR model to the mixing coefficients. For this case, the two-mode model for steady state may be written as

$$C_{A,m,\text{in}} - \langle C_A \rangle = k\tau \hat{R}(\langle C_A \rangle) \quad (104)$$

$$C_{A,m} - \langle C_A \rangle = \delta_2 C_{A,m}^{\text{in}} - \delta_1 C_{A,m} \quad (105)$$

By combining the above two equations, it is easily seen that, provided $1 + k\tau \frac{dR}{dC_A}(\langle C_A \rangle) \neq 0$

$$\frac{\partial C_{A,m}}{\partial \delta_1} \Big|_{\delta_1 = \delta_2 = 0} = -C_{A,m} < 0 \quad (106)$$

$$\frac{\partial C_{A,m}}{\partial \delta_2} \Big|_{\delta_1 = \delta_2 = 0} = C_{A,m}^{\text{in}} > 0 \quad (107)$$

Thus, the exit cup-mixing concentration decreases (or conversion increases) with the first mixing coefficient while the converse is true for the second mixing coefficient. We also note that since $C_{A,m}$ is usually much smaller (especially at high conversions) compared to $C_{A,m}^{\text{in}}$, the impact of the first mixing coefficient on the exit conversion is smaller compared to the second mixing coefficient. Finally, we note that the condition $1 + k\tau \frac{dR}{dC_A}(\langle C_A \rangle) \neq 0$ is satisfied for monotone kinetics (reaction rate increasing with concentration), but it may be violated for autocatalytic kinetics, for which there can be multiple steady states. We do not examine here the impact of mixing on the region of multiple solutions, as it is not the focus of this work.

Before moving on to the next example, we pause to reflect on the physical meaning of the two mixing coefficients. At first glance, they just seem to be dimensionless quantities, but a closer inspection reveals that both of these coefficients can be interpreted in the traditional reaction engineering terminology. The local equation expresses $\langle C \rangle$ in terms of C_m as

$$\langle C \rangle = (1 + \delta_1)C_m - \delta_2 C_m^{\text{in}} \quad (108)$$

For $\delta_2 = 0$, we have

$$C_m = \frac{\langle C \rangle}{1 + \delta_1} \quad (109)$$

This means that the mean residence time for our system gets modified by a factor of $(1 + \delta_1)$ compared to the ideal CSTR. Similarly, when $\delta_1 = 0$, the reaction rate is evaluated

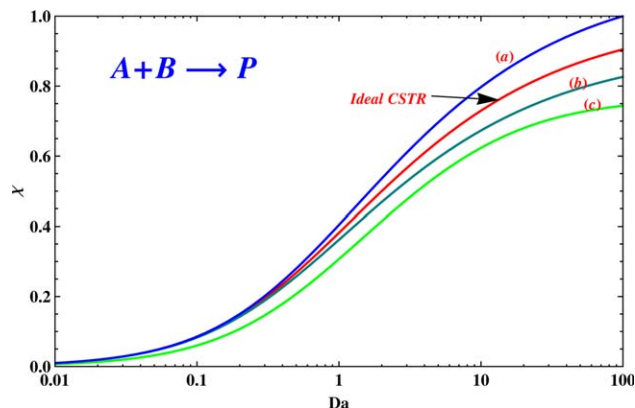


Figure 4. Impact of mixing effects on conversion for a bimolecular reaction.

Case (a) corresponds to $\delta_1 = \delta_{2A} = \delta_{2B} = -0.1$, case (b) to $\delta_1 = \delta_{2A} = \delta_{2B} = 0.1$, and case (c) to $\delta_1 = -0.15$, $\delta_{2A} = -0.2$, and $\delta_{2B} = 0.2$. [Color figure can be viewed in the online issue, which is available at [wileyonlinelibrary.com](http://www.wileyonlinelibrary.com).]

at lower or higher concentrations than the measured mixing-cup concentration depending on the sign of δ_2 (this follows from the fact that the only rate terms in the model are of the form $R(\langle C \rangle)$ and in this case $\langle C \rangle = C_m - \delta_2 C_m^{\text{in}}$). For instance, if $\delta_2 < 0$ and if kinetics is monotone, the volume-averaged concentration and, hence, the reaction rate are higher compared to the ideal CSTR. In other nonlinear reactions, departures from the ideal case could be much more drastic.

Now, we consider the second example: a bimolecular reaction between species A and B. In this case, averaged model for the same system (after regularization) is given by

$$\begin{aligned} C_{A,m,\text{in}} - C_{A,m} &= \tau k \langle C_A \rangle \langle C_B \rangle \\ C_{B,m,\text{in}} - C_{B,m} &= \tau k \langle C_A \rangle \langle C_B \rangle \\ C_{A,m} - \langle C_A \rangle &= \delta_{2A} C_{A,m}^{\text{in}} - \delta_1 C_{A,m} \\ C_{B,m} - \langle C_B \rangle &= \delta_{2B} C_{B,m}^{\text{in}} - \delta_1 C_{B,m} \end{aligned} \quad (110)$$

We solve for the conversion of the system in four simple cases that illustrate the usefulness of our approach and plot the results as shown in Figure 4. When both the mixing coefficients are zero, we have an ideal CSTR with perfect mixing. To introduce finite mixing, we consider a few two-cell arrangements. When both A and B arrive in the same cell, all the mixing coefficients are found to be negative when the exit stream comes out of the other cell and positive when the exit is from the same cell. In the specific example, we have considered all δ_i 's are taken to be -0.1 in (a) and 0.1 in (b), respectively. This is regardless of the relative dilution of the feed. As we noted, the second mixing coefficient is likely to have a stronger effect on the conversion. Hence, arrangement (a) with a negative second mixing coefficient leads to an increase in conversion as compared to the classical CSTR case. Likewise arrangement (b) leads to a decrease in conversion. The other interesting two cell case is when the two reactants enter different cells. Now, the relative dilutions start playing a role. Our calculations show that for arrangement (c) ($\delta_1 = -0.15$, $\delta_{2A} = -0.2$, and $\delta_{2B} = 0.2$), conversion decreases if A is dilute and A and B are fed in two different cells with the product taken out from the cell in which B is fed.

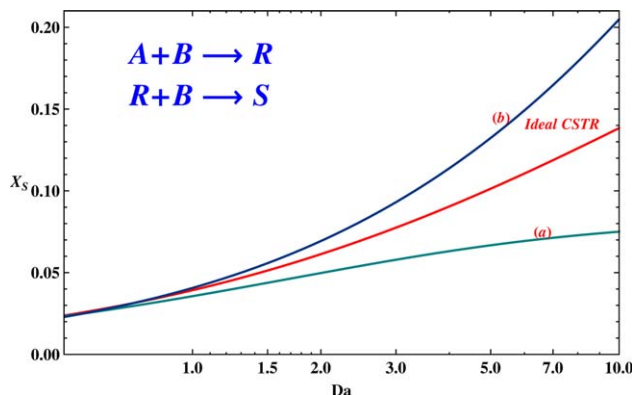
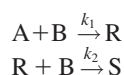


Figure 5. Impact of mixing effects on the yield of product S in a competitive-consecutive reaction scheme.

Case (a) corresponds to $\delta_1=0.18$, $\delta_{2A}=-0.2$, and $\delta_{2B}=0.2$, whereas case (b) corresponds to $\delta_1=-0.18$, $\delta_{2A}=0.2$, and $\delta_{2B}=-0.2$. [Color figure can be viewed in the online issue, which is available at wileyonlinelibrary.com.]

The third and final example we consider is that of competitive-consecutive kinetics described by



We consider the case of stoichiometric feeding of A and B ($C_{Am,in} = C_{Bm,in}$) and the case when the first reaction is very fast compared to the second. In particular, we study the case when $k_1 = 30k_2$. We only need three mixing coefficients, namely, δ_1 , δ_{2A} , and δ_{2B} . After dimension-reduction, the steady-state balances for this system can be written as

$$\begin{aligned} C_{Am,in} - C_{Am} &= \tau k_1 \langle C_A \rangle \langle C_B \rangle \\ C_{Bm,in} - C_{Bm} &= \tau k_1 \langle C_A \rangle \langle C_B \rangle + \tau k_2 \langle C_R \rangle \langle C_B \rangle \\ -C_{Rm} &= -\tau k_1 \langle C_A \rangle \langle C_B \rangle + \tau k_2 \langle C_R \rangle \langle C_B \rangle \\ -C_{Sm} &= -\tau k_2 \langle C_R \rangle \langle C_B \rangle \\ C_{Am} - \langle C_A \rangle &= \delta_{2A} C_{Am,in} - \delta_1 C_{Am} \\ C_{Bm} - \langle C_B \rangle &= \delta_{2B} C_{Am,in} - \delta_1 C_{Bm} \\ C_{Rm} - \langle C_R \rangle &= -\delta_1 C_{Bm} \\ C_{Sm} - \langle C_S \rangle &= -\delta_1 C_{Bm} \end{aligned} \quad (111)$$

Let us define $y_J = \frac{C_{Jm}}{C_{Jm,in}}$ where $J = A, B, R$, or S . We want to study the effect of changing Damköhler number on the selectivity (or yield) of product S. The selectivity, X_S is defined as the moles of B in the feed that is converted to S divided by the total moles of B reacted. From stoichiometry of the reactions, we then have $X_S = \frac{2y_S}{2y_S + y_R}$. We define the Da using the rate constant of the faster reaction. Thus, $Da = k_1 C_{Am,in} \tau$. We can simplify the analysis here by finding the invariants

$$\begin{aligned} y_R &= 1 - 2y_A + y_B \\ y_S &= y_A - y_B \end{aligned} \quad (112)$$

Our results are shown in Figure 5. The cases (a) and (b) in Figure 5 correspond to

$$\begin{aligned} (a) \delta_1 &= 0.18, \delta_{2A} = -0.2, \delta_{2B} = 0.2, \text{ and} \\ (b) \delta_1 &= -0.18, \delta_{2A} = 0.2, \delta_{2B} = -0.2 \end{aligned}$$

Both of these cases correspond to feeding A and B, so that A is concentrated, yet the arrangement of the exit affects the selectivity of S. Thus, it can be readily seen that depending on the manner of feeding of the reactants, the yield of the product S can be enhanced or decreased compared to the ideal CSTR case.

Summary and Discussion

As stated in the “Introduction” section, the main goal of this work was to investigate the spectral properties of the operators appearing in the mathematical models of the loop and recycle reactors and use these properties to obtain low-dimensional averaged models of these systems. We have shown that when the circulation or recycle flow rate is much larger compared to the feed flow rate, which is the case in most practical systems, the leading order convection operator with loop boundary condition has a real eigenvalue that approaches zero as the ratio $\epsilon = (q_F/Q_R) \rightarrow 0$. We have exploited this scale separation to obtain accurate reduced order models of these systems. From a physical point of view, such systems are well mixed, but the mixing is imperfect and macromixing effects due to the entrance and exit of various feed and product streams at different flow rates and concentrations cause a departure from the assumption of the ideal CSTR. These finite mixing effects appear in the reduced order models through the two mixing coefficients. Of these the first mixing coefficient depends only on the internal flow structure and connectivity of the system. It is, therefore, the same for all species. On the other hand, the second mixing coefficient depends both on the internal flow structure and on how different reactant species enter the system at different relative flow rates and concentrations. As the second mixing coefficient depends linearly on inlet concentration of the species, it is zero for all the intermediate species. In addition, the second mixing coefficient has a stronger influence on the system behavior compared to the first mixing coefficient. We have provided examples illustrating the use of the reduced order models in predicting conversion, yield, and selectivity in single and multiple reactions. These examples illustrate how the various macroscopically observable parameters of the system (e.g., the arrangement of cells/loops, position of inlets and exits, concentrations, and flow rates of various feed streams) can collectively affect the system, and how this can be analyzed and controlled in a simple manner through the two mixing coefficients. Our low-dimensional description not only reduces the computational effort required it also gives a better intuitive picture in terms of measurable quantities.

This work was confined to specific arrangements of discrete cells or continuous systems that correspond to circulant matrices or loop operators. However, the same methodology can be applied to more general arrangements of discrete cells (where each cell interacts with every other cell) or to the corresponding continuum case. These more general arrangements may be useful for modeling real stirred reactors more effectively. Usually in such systems, there are a few dominant circulatory flows which could be modeled as coexisting loops that interact. Thus, the arrangement of interacting loops may capture the geometry of the manner in which

different species mix in a real stirred tank reactor. It can be shown that a scale separation (and a zero eigenvalue) does exist for a lot of such interesting, general operators but exploiting it to derive a low-dimensional model is difficult. For example, in the discrete case, the matrix is not circulant but has zero row and column sum. Similarly, our approach can easily be generalized to the case in which the auxiliary flows are time dependent but still much smaller compared to the main flow. The present approach may also be combined with an earlier approach⁹ to include molecular diffusion effects. We also remark that although we restricted ourselves here to isothermal reactors and monotone kinetics, our formalism extends readily to these cases as well. Here, the low-dimensional models can greatly aid the study of bifurcation features of these systems. These and other extensions will be pursued in future work.

Acknowledgments

This work is dedicated to late Professor Neal R. Amundson, a distinguished teacher, mentor, role model and continuous source of inspiration. It was supported by a grant from the Robert A. Welch foundation, grant #E-1152.

Notation

Roman letters

- A_c = cross-sectional area of the tube
- c = dimensionless concentration
- C = concentration (dimensional)
- C_{in} = inlet fluid concentration (dimensional)
- D_e = axial dispersion coefficient
- D_a = Damköhler number
- L = length of the loop reactor
- P_e = axial Peclet number
- q_F = total inlet or exit flow rate (dimensional)
- Q_R = loop circulation rate (dimensional)
- $r(c)$ = dimensionless reaction rate
- $R'(C)$ = reaction rate (dimensional)
- t' = time (dimensional)
- t = dimensionless time
- $\langle u \rangle$ = average fluid velocity
- V_c = volume of discrete cell
- x' = coordinate along the length of the reactor (dimensional)
- x = dimensionless coordinate along the length of the reactor

Greek letters

- α_i = fractional inlet or exit flow rate of stream
- ϵ = ratio of total feed flow rate to circulation rate ($= q_F/Q_R$)
- δ_i = mixing coefficient

Subscripts and superscripts

- m = cup-mixing
- in = inlet conditions

Literature Cited

- Schmeal WR, Amundson NR. The effect of recycle on a linear reactor. *AIChE J.* 1966;12:1202–1211.
- Luss D, Amundson NR. Stability of loop reactors. *AIChE J.* 1967;13:279–290.
- Nagiev MF. The Theory of Recycle Processes in Chemical Engineering. New York: Macmillan, 1964.
- Amundson NR. Mathematical Methods in Chemical Engineering, Vol. 1: Matrices. NJ: Prentice Hall, 1966.
- Ramkrishna D, Amundson NR. Linear Operator Methods in Chemical Engineering. NJ: Prentice Hall, 1985.
- Ramkrishna D, Amundson NR. Mathematics in chemical engineering: a 50 year introspection. *AIChE J.* 2004;50:7–23.

- Kevrekidis IG. Matrices are forever. *Chem Eng Sci.* 1995;50:4005–4025.
- Aldrovandi R. Special Matrices of Mathematical Physics. World Scientific: Singapore, 2001.
- Bhattacharya M, Harold MP, Balakotaiah V. Low-dimensional models for homogeneous stirred tank reactors. *Chem Eng Sci.* 2004;59:5587–5596.
- Balakotaiah V, Chang H-C. Hyperbolic homogenized models for thermal and solutal dispersion. *SIAM J Appl Math.* 2003;63:1231–1258.
- Ratnakar R, Balakotaiah V. Exact averaging of laminar dispersion. *Phys Fluids.* 2011;23:023601–1–23.
- Chakraborty S, Balakotaiah V. Spatially averaged multiscale models for chemical reactors. *Adv Chem Eng.* 2005;30:205–297.

Appendix: A

Circulant Matrices

A circulant matrix $\text{circ}(a_1, a_2, \dots, a_N)$ denotes the matrix

$$\begin{bmatrix} a_1 & a_2 & \dots & \dots & \dots & a_N \\ a_N & a_1 & \dots & \dots & \dots & a_{N-1} \\ \vdots & & \ddots & & & \vdots \\ \vdots & & & \ddots & & \vdots \\ \vdots & & & & \ddots & \vdots \\ a_2 & \dots & \dots & \dots & \dots & a_1 \end{bmatrix}$$

Any row of this matrix can be obtained by rotating the elements of the previous row to the right. It is a special case of a Toeplitz matrix (for which elements on all the diagonals are constants). In this work, we have used several properties of these matrices, in particular their Fourier transform and inverse. The Fourier transform on these matrices is a simple Z_n -transform in terms of the entries a_j which gives the matrix eigenvalue λ_j as

$$\lambda_j = \sum_{l=1}^N a_l e^{i(\frac{2\pi}{N})jl} = \sum_{l=1}^N a_l \omega^{jl} \quad (\text{A1})$$

where ω is the N th root of unity. All the right and left eigenvectors are given as

$$\mathbf{u}_j = \frac{1}{\sqrt{N}} [1, \omega^{-j}, \omega^{-2j}, \dots, \omega^{-(N-1)j}] \quad (\text{A2})$$

Of course, the normalization factor $\frac{1}{\sqrt{N}}$ can be changed if desired, for example, in this work, we have kept $\frac{1}{N}$ in the left eigenvector so that the normalization factor for the right eigenvector becomes 1.

We note that if the row entries sum to zero (i.e., $a_1 + a_2 + \dots + a_N = 0$), we have $\lambda_0 = 0$, and the corresponding eigenvector $\mathbf{u}_0 = \frac{1}{\sqrt{N}} [1, 1, 1, \dots, 1]$.

Appendix: B

A Sample Calculation of Mixing Coefficients

We show the details of calculation for (97) and (98) from one of our examples of discrete cell models in which we have the inlet in cell 1 and exit in cell m . In this case, the matrices α_{in} and α_c become

$$\alpha_{\text{in}} = \begin{bmatrix} 1 & 0 & \cdots & 0 \\ 0 & 0 & \cdots & 0 \\ \vdots & \vdots & \ddots & \vdots \\ 0 & 0 & \cdots & 0 \end{bmatrix} \quad (\text{B1})$$

and

$$\alpha_{\text{e}} = \begin{bmatrix} 1 & 0 & 0 & \cdots & \cdots & 0 & 0 \\ -1 & 1 & 0 & \cdots & \cdots & 0 & 0 \\ \vdots & \vdots & \vdots & \vdots & \vdots & \vdots & \vdots \\ 0 & 0 & \cdots & -1 & 1 & \cdots & 0 \\ 0 & 0 & \cdots & 0 & \cdots & 0 & 0 \\ \vdots & \vdots & \cdots & \vdots & \cdots & \vdots & \vdots \\ 0 & 0 & \cdots & 0 & \cdots & 0 & 0 \end{bmatrix} \quad (\text{B2})$$

In the matrix α_{e} , the last nonzero row is the m th row and all the rows except the first and all the columns except the m th sum to zero. The first row and the m th column sum to unity.

We proceed to evaluate δ_2 as outlined in the section on dimension reduction. To that end, we first need to solve

$$\mathbf{A}\mathbf{z} = N \left\{ (1, 0, 0, \dots, 0)^T - \frac{\mathbf{y}_0}{N} \right\} \quad (\text{B3})$$

Let $\mathbf{z} = (z_1, z_2, z_3, \dots, z_N)^T$. Then, explicitly writing the linear system, we have

$$\begin{aligned} z_1 - z_N &= 1 - \frac{1}{N} \\ -z_1 + z_2 &= -\frac{1}{N} \\ -z_2 + z_3 &= -\frac{1}{N} \\ &\vdots \\ -z_{N-1} + z_N &= -\frac{1}{N} \end{aligned} \quad (\text{B4})$$

Evidently, the above system is not linearly independent as adding them up gives $0 = 0$. We actually have only $(N - 1)$ linearly independent equations. So, to solve it, we remove any one equation and add the consistency condition given by

$$z_1 + z_2 + z_3 + \dots + z_N = 0 \quad (\text{B5})$$

as the final equation. Solving the above system is trivial. So we can easily use our formulas derived for general discrete systems now to calculate δ_2 . We obtain

$$\delta_2 = \epsilon \left(\frac{N - 2m + 1}{2N} \right) \quad (\text{B6})$$

Similarly, one can obtain δ_1 , which in this case turns out to be the same as δ_2 .

Manuscript received Dec. 19, 2012, and revision received Feb. 28, 2013.